

Site-specific Ligand Variation in Manganese–Oxide Cubane Complexes, and Unusual Magnetic Relaxation Effects in $[\text{Mn}_4\text{O}_3\text{X}(\text{OAc})_3(\text{dbm})_3]$ ($\text{X} = \text{N}_3^-$, OCN^- ; Hdbm = dibenzoylmethane)

Michael W. Wemple,^a David M. Adams,^b Karl S. Hagen,^c Kirsten Folting,^a David N. Hendrickson*^b and George Christou*^a

^a Department of Chemistry and the Molecular Structure Center, Indiana University, Bloomington, IN 47405-4001, USA

^b Department of Chemistry-0358, University of California at San Diego, La Jolla, CA 92093-0358, USA

^c Department of Chemistry, Emory University, Atlanta, GA 30322, USA

Treatment of $[\text{Mn}_4\text{O}_2(\text{OAc})_6(\text{py})_2(\text{dbm})_2]$ **1** (py = pyridine, Hdbm = dibenzoylmethane) in hot MeCN with Me_3SiX ($\text{X} = \text{N}_3^-$, OCN^-) yields $[\text{Mn}_4\text{O}_3\text{X}(\text{OAc})_3(\text{dbm})_3]$ containing extremely rare $\eta^1, \mu_3\text{-N}_3^-$ or $-\text{OCN}^-$ groups; alternating-current magnetic susceptibility studies reveal unusual magnetic relaxation effects and indicate these species to be the newest and smallest examples yet of truly molecular magnets.

We have for some time^{1,2} been interested in complexes containing the $[\text{Mn}^{\text{III}}_3\text{Mn}^{\text{IV}}(\mu_3\text{-O})_3(\mu_3\text{-Cl})]^{6+}$ distorted cubane core both as models for the tetranuclear water oxidation centre near Photosystem II in green plants and because they possess unusual magnetic properties. These complexes possess a ground state with a large spin ($S = 9/2$), a result of spin frustration effects within the pyramidal 3Mn^{III} , Mn^{IV} core of C_{3v} symmetry; antiferromagnetic coupling within the $\text{Mn}^{\text{III}}/\text{Mn}^{\text{IV}}$ pairs dominates and causes the three Mn^{III} spins to ferromagnetically align, yielding a ground state with $S = 6 - 3/2 = 9/2$. These complexes are prepared by disproportionation of a Mn^{III} precursor; thus, treatment of $[\text{Mn}_4\text{O}_2(\text{OAc})_6(\text{py})_2(\text{dbm})_2]$ **1** (4Mn^{III}) with NBu_4Cl^2 or Me_3SiCl^3 in hot MeCN or CH_2Cl_2 yields $[\text{Mn}_4\text{O}_3\text{Cl}(\text{OAc})_3(\text{dbm})_3]$ **2** (3Mn^{III} , Mn^{IV}). A related procedure⁴ employing Me_3SiBr yields $[\text{Mn}_4\text{O}_3\text{Br}(\text{OAc})_3(\text{dbm})_3]$ **3**, which also has an $S = 9/2$ ground state. We have wondered whether pseudohalides could also be incorporated into the $[\text{Mn}_4\text{O}_3\text{X}]^{6+}$ core, for example N_3^- , OCN^- , and others. However, one would normally expect to see the two mentioned ions in a monoatomic, triply-bridging (η^1, μ_3) mode, the latter being extremely rare, and this suggests that reactions of **1** with Me_3SiN_3 or Me_3SiNCO might not be predicted to give products analogous to **2** and **3**. Nevertheless, we herein report that these reactions do indeed give the products $[\text{Mn}_4\text{O}_3\text{X}(\text{OAc})_3(\text{dbm})_3]$ ($\text{X} = \text{N}_3^-$ **4**, OCN^- **5**), providing a convenient route into rare η^1, μ_3 structural chemistry of N_3^- and OCN^- . We also show that **4** and **5** display magnetic properties that are remarkable for molecular species.

Treatment of **1** with ≈ 1.5 equivalents of Me_3SiX ($\text{X} = \text{N}_3^-$, N-bound OCN^-) in hot MeCN gives crystalline products **4** and **5** in 12 and 27% yields, respectively, based on total Mn; recrystallization from $\text{CH}_2\text{Cl}_2\text{-MeCN}$ or $\text{CH}_2\text{Cl}_2\text{-MeCN-Et}_2\text{O}$ (for **4** and **5**, respectively) gives X-ray quality crystals.[†] Since there has been a disproportionation, the true yields are somewhat higher. The structures of **4** and **5** (Fig. 1) consist of a $[\text{Mn}_4\text{O}_3\text{X}]^{6+}$ core with peripheral ligation provided by three bridging AcO^- and three chelating dbm^- groups. On the basis of structural parameters and Jahn–Teller distortions at the near-octahedral Mn^{III} (d^4 , high-spin) centres, $\text{Mn}(2)$, $\text{Mn}(3)$ and $\text{Mn}(4)$ are concluded to be the Mn^{III} ions and $\text{Mn}(1)$ to be the Mn^{IV} ion. The remarkable structural feature of both complexes is the $\eta^1, \mu_3\text{-N}_3^-$ or $-\text{OCN}^-$ at one vertex, bridging the Mn^{III} ions and lying on the Jahn–Teller elongation axes; as a result, the Mn–N distances are rather long, 2.302(9)–2.329(9) and 2.322(8)–2.403(8) Å for **4** and **5**, respectively. In **2** and **3**, the Mn–halide bonds are even longer, ≈ 2.65 and ≈ 2.80 Å, respectively, which also makes the Mn–X–Mn angles ($\approx 76^\circ$ in **2** and $\approx 72^\circ$ in **3**) much more acute than in **4** or **5** ($\approx 86^\circ$). In addition, the $\text{Mn}^{\text{III}}\cdots\text{Mn}^{\text{III}}$ distances in **4** and **5** contract slightly compared with **2** (≈ 3.19 vs. 3.25 Å), as do the $\text{Mn}^{\text{III}}\text{-O-Mn}^{\text{III}}$ angles (≈ 112 vs. $\approx 115^\circ$). There are only three previous, structurally confirmed examples of $\eta^1, \mu_3\text{-N}_3^-$ groups in molecular species: $[\text{Pt}_4(\text{N}_3)_4\text{Me}_{12}]$,⁵ $[\text{Ti}_3(\text{N}_3)_4(\text{NH})(\text{NMe})_6]$ ⁶

and $[\text{Ni}_4(\text{N}_3)_4(\text{dbm})_4(\text{EtOH})_4]$,⁷ $\eta^1, \mu_3\text{-OCN}^-$ groups are even rarer, being seen previously only in $[\text{Mn}_4(\text{NCO})_2(\text{CH}_2\text{Bu}^t)_2\text{-}\{\text{OC}(\text{CH}_2\text{Bu}^t)\text{N}(\text{SiMe}_3)\}_4]$.⁸

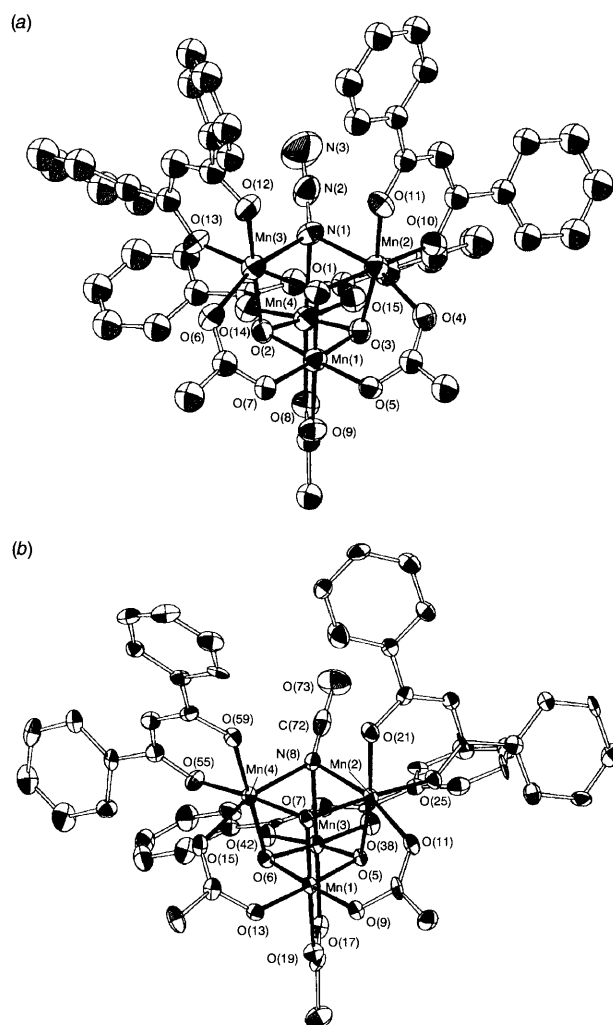


Fig. 1 ORTEP representation of complex **4** (a) and **5** (b) at the 50% probability level. Selected distances (Å) and angles ($^\circ$) for **4** are: $\text{Mn}(1)\cdots\text{Mn}(2)$ 2.801(2), $\text{Mn}(1)\cdots\text{Mn}(3)$ 2.783(2), $\text{Mn}(1)\cdots\text{Mn}(4)$ 2.796(2), $\text{Mn}(2)\cdots\text{Mn}(3)$ 3.164(2), $\text{Mn}(2)\cdots\text{Mn}(4)$ 3.209(2), $\text{Mn}(3)\cdots\text{Mn}(4)$ 3.195(2), $\text{Mn}(2)\text{-N}(1)$ 2.302(9), $\text{Mn}(3)\text{-N}(1)$ 2.318(9), $\text{Mn}(4)\text{-N}(1)$ 2.329(9), $\text{Mn}(2)\text{-N}(1)\text{-Mn}(3)$ 86.5(3), $\text{Mn}(2)\text{-N}(1)\text{-Mn}(4)$ 87.7(3), $\text{Mn}(3)\text{-N}(1)\text{-Mn}(4)$ 86.9(3). For **5**: $\text{Mn}(1)\cdots\text{Mn}(2)$ 2.781(2), $\text{Mn}(1)\cdots\text{Mn}(3)$ 2.806(2), $\text{Mn}(1)\cdots\text{Mn}(4)$ 2.794(2), $\text{Mn}(2)\cdots\text{Mn}(3)$ 3.204(2), $\text{Mn}(2)\cdots\text{Mn}(4)$ 3.209(2), $\text{Mn}(3)\cdots\text{Mn}(4)$ 3.162(2), $\text{Mn}(2)\text{-N}(8)$ 2.403(8), $\text{Mn}(3)\text{-N}(8)$ 2.344(8), $\text{Mn}(4)\text{-N}(8)$ 2.322(8), $\text{Mn}(2)\text{-N}(8)\text{-Mn}(3)$ 84.9(3), $\text{Mn}(2)\text{-N}(8)\text{-Mn}(4)$ 85.5(3), $\text{Mn}(3)\text{-N}(8)\text{-Mn}(4)$ 85.3(3).

Solid samples of complexes **4** and **5** were studied by DC magnetic susceptibility measurements in the temperature range 2–300 K. The data are presented in Fig. 2 as effective magnetic moment (μ_{eff}) per Mn_4 vs. temperature plots; also shown are the fits of the data (solid lines) to the theoretical expression derived elsewhere for a $\text{Mn}^{\text{III}}_3\text{Mn}^{\text{IV}}$ pyramid of C_{3v} symmetry.¹ The fitting parameters in the format **4/5** were (using the $\hat{H} = -2J\hat{S}_i\hat{S}_j$ convention): $J_{34} = J(\text{Mn}^{\text{III}}\dots\text{Mn}^{\text{IV}}) = -18.3/-25.7 \text{ cm}^{-1}$, $J_{33} = J(\text{Mn}^{\text{III}}\dots\text{Mn}^{\text{III}}) = 10.2/8.1 \text{ cm}^{-1}$ and $g = 1.94/1.89$. These parameters show that **4** and **5** both have $S = 9/2$ ground states. The exchange parameters J_{34} and J_{33} may be compared with those for **2** (-28.4 and $+8.3 \text{ cm}^{-1}$, respectively³); whereas the OCN^- ion causes no noticeable effect on the exchange parameters *vis-à-vis* the Cl^- complex **2**, the N_3^- ion causes more significant changes, weakening the antiferromagnetic J_{34} $\text{Mn}^{\text{III}}\dots\text{Mn}^{\text{IV}}$ interaction and strengthening the ferromagnetic J_{33} $\text{Mn}^{\text{III}}\dots\text{Mn}^{\text{III}}$ interaction. It is relevant to note that $\eta^1, \mu_3\text{-N}_3^-$ mediates a ferromagnetic interaction between the Ni^{II} ions in $[\text{Ni}_4(\text{N}_3)_4(\text{dbm})_4(\text{EtOH})_4]$ ($J = +11.9 \text{ cm}^{-1}$).⁷ No magnetic data were reported for the only previous example of a $\eta^1, \mu_3\text{-OCN}^-$.⁸ Also, the ability of N_3^- to influence the exchange interaction between two metal centres it does not bridge parallels that in the $[\text{Mn}_2\text{O}(\text{O}_2\text{CR})_2\text{X}_2(\text{bpy})_2]$ ($\text{X} = \text{Cl}^-, \text{N}_3^-$) dinuclear systems,⁹ where terminal N_3^- groups weaken the antiferromagnetic interaction between the Mn^{III} centres, to the point of J becoming positive.

Complexes **4** and **5** display unusual magnetic relaxation effects. AC magnetic susceptibility data were collected for both complexes in the 1.7–50 K range with zero DC field and with a 1.0 G AC field oscillating at 250, 499 or 997 Hz. In both cases, there is a plateau in the $\chi_M' T$ vs. T plot in the ≈ 10 –50 K range, where χ_M' is the in-phase AC susceptibility. The plateau for each complex is consistent with a $S = 9/2$ ground state. However, at temperatures below ≈ 3 K, $\chi_M' T$ drops off abruptly for each complex. At these low temperatures, the magnetization of complexes **4** and **5** cannot keep in phase with the oscillating field, and an out-of-phase AC signal (χ_M'') appears at the temperature where the in-phase component begins to decrease (Fig. 3). Similar frequency-dependent AC signals were observed^{10–12} for $[\text{Mn}_{12}\text{O}_{12}(\text{O}_2\text{CR})_{16}(\text{H}_2\text{O})_4]$ ($\text{R} = \text{Me}, \text{Et}$) complexes; the Mn_{12} complexes exhibit maxima in the χ_M' signal at *ca.* 6–8 K, compared to 1.6–2.0 K for complexes **4** and **5**. This type of relaxation has only been seen previously for the Mn_{12} and their one-electron-reduced complexes. It has been

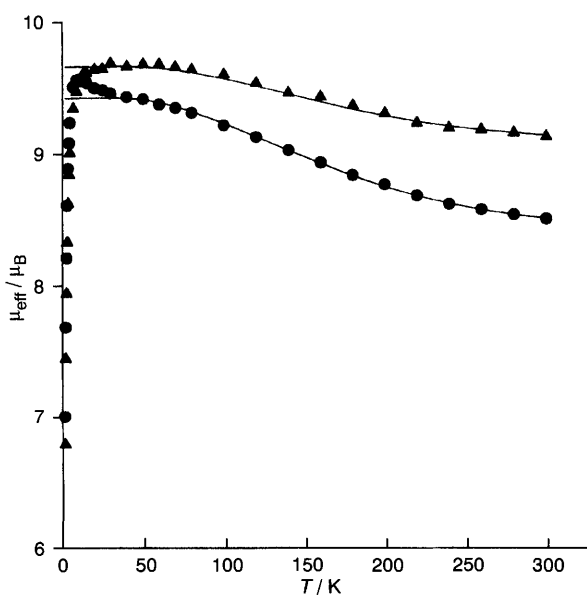


Fig. 2 Plots of effective magnetic moment (μ_{eff}) per Mn_4 vs. T for complexes **4** (\blacktriangle) and **5** (\bullet). The solid lines are fits of the data to the appropriate theoretical expression; see text for fitting parameters.

shown that the individual Mn_{12} complexes are behaving as magnetizable magnets (*i.e.* hysteresis loops are seen at 2.2 K). There is appreciable magnetic anisotropy due to zero-field interactions ($D \approx 0.5 \text{ cm}^{-1}$ in $D\hat{S}_z^2$) in the large-spin ($S = 9$ or 10) ground states of the Mn_{12} complexes. For the present $\text{Mn}^{\text{III}}_3\text{Mn}^{\text{IV}}$ complexes **4** and **5**, the $S = 9/2$ ground state experiences a $D = 0.3$ – 0.5 cm^{-1} axial zero-field splitting as determined by magnetization vs. field studies. Unlike the Mn_{12} complexes which have larger barriers to relaxation, **4** and **5** do not exhibit hysteresis loops at 1.7 K, the lowest temperature we can attain, indicating that the relaxation rate at this temperature is too fast for the timescale of this DC experiment. Lower temperatures would be required for hysteresis to be exhibited. Finally, recent results establish that the other known $[\text{Mn}_4\text{O}_3\text{X}]^{6+}$ complexes also exhibit very similar magnetic relaxation behaviour.¹³ Thus, these Mn_4 complexes are the second family of complexes that have been found to function as molecular magnets (*i.e.* behaviour arising from the intrinsic properties of single, isolated molecules rather than extended lattices of interacting molecules), and show that this important property can be obtained in molecules with a metal nuclearity as low as four.

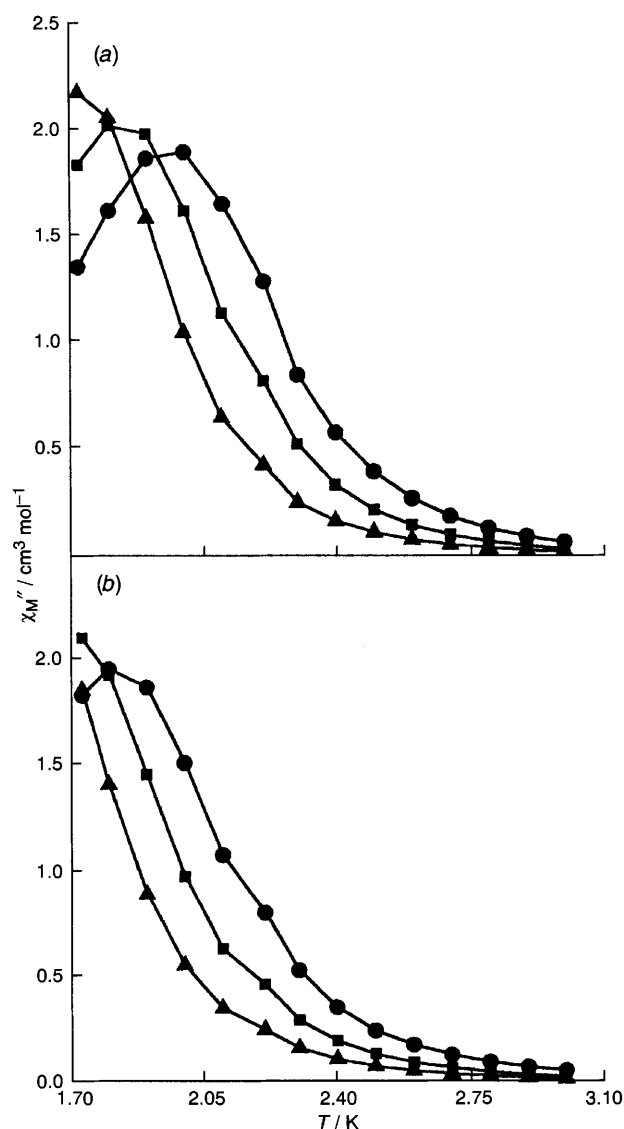


Fig. 3 Plot of the out-of-phase component of the molar AC magnetic susceptibility (χ_M'') vs. T for polycrystalline samples of complexes **4** (a) and **5** (b). Data were collected in zero DC field and 1.0 G (10^{-4} T) AC field at three frequencies: (\bullet) 997, (\blacksquare) 499 and (\blacktriangle) 250 Hz. The lines are visual guides.

This work was supported by the US National Institutes of Health and the National Science Foundation.

Received, 18th April 1995; Com. 5102418H

Footnotes

† Analytical data (C, H, N) for the vacuum-dried solids were satisfactory.
‡ *Crystal data* for 4-MeCN: C₅₃H₄₅Mn₄N₄O₁₅, *M* = 1197.69, triclinic, *P*1, *a* = 10.052(1), *b* = 14.404(2), *c* = 19.667(2) Å, α = 73.86(1), β = 81.76(1), γ = 70.70(1)°, *V* = 2577.4(5) Å³, *Z* = 2, *D*_c = 1.543 gm cm⁻³, λ = 1.54178 Å, *T* = 173 K, 4.7 < 2θ < 90°. The structure was solved using SHELXL-92. A total of 4121 independent reflections were refined using full-matrix, least squares on *F*² to final *R* indices [*I* > 2σ(*I*)] or *R*₁ = 0.0653 and *wR*₂ = 0.1566. An absorption correction was applied. In the final refinement cycles, Mn, O, and N of molecule 4 were refined anisotropically as well as one of the carbon atoms of the solvent molecule. All other atoms were refined isotropically, and H atoms were included in calculated positions with fixed thermal parameters.

§ *Crystal data* for 5·CH₂Cl₂: C₅₃H₄₄Cl₂Mn₄NO₁₆, *M* = 1241.59, monoclinic, *P*2₁/*n*, *a* = 13.918(2), *b* = 17.789(3), *c* = 21.448(4) Å, β = 98.50(1)°, *V* = 5251.76 Å³, *Z* = 4, *D*_c = 1.570 gm cm⁻³, λ = 0.71069 Å, *T* = -172 °C, 6 ≤ 2θ ≤ 45°, *R*(*R*_w) = 0.0792(0.0709) for 4739 unique reflections with *F* > 3σ(*F*). The structure was solved by MULTAN and Fourier techniques, and refined on *F* by full-matrix, least-squares analysis. The asymmetric unit contains one molecule of 5 and disordered solvent molecules. The latter were eventually defined as two half-weight molecules of dichloromethane. All non-hydrogen atoms (except for the solvent atoms) were refined anisotropically, and H atoms were included in calculated positions with fixed thermal parameters. Atomic coordinates, bond lengths and angles, and thermal parameters have been deposited at the Cambridge Crystallographic Data Centre. See Information for Authors, Issue No. 1.

References

- 1 D. N. Hendrickson, G. Christou, E. A. Schmitt, E. Libby, J. S. Bashkin, S. Wang, H.-L. Tsai, J. B. Vincent, P. D. W. Boyd, J. C. Huffman, K. Folting, Q. Li and W. E. Streib, *J. Am. Chem. Soc.*, 1992, **114**, 2455; E. A. Schmitt, L. Noodleman, E. J. Baerends and D. N. Hendrickson, *J. Am. Chem. Soc.*, 1992, **114**, 6109; M. W. Wemple, H.-L. Tsai, K. Folting, D. N. Hendrickson and G. Christou, *Inorg. Chem.*, 1993, **32**, 2025.
- 2 S. Wang, K. Folting, W. E. Streib, E. A. Schmitt, J. K. McCusker, D. N. Hendrickson and G. Christou, *Angew. Chem., Int. Ed. Engl.*, 1991, **30**, 305.
- 3 S. Wang, H.-L. Tsai, J. C. Huffman, K. Folting, D. N. Hendrickson and G. Christou, submitted for publication.
- 4 S. Wang, H.-L. Tsai, W. E. Streib, G. Christou and D. N. Hendrickson, *J. Chem. Soc., Chem. Commun.*, 1992, 1427.
- 5 M. Atam and U. Müller, *J. Organomet. Chem.*, 1974, **71**, 435.
- 6 M. E. Gross and T. Siegrist, *Inorg. Chem.*, 1992, **31**, 4898.
- 7 M. A. Halcrow, J. C. Huffman and G. Christou, *Angew. Chem., Int. Ed. Engl.*, 1995, **34**, 889; M. A. Halcrow, J.-S. Sun, J. C. Huffman and G. Christou, *Inorg. Chem.*, in the press.
- 8 S. U. Koschmieder, G. Wilkinson, B. Hussain-Bates and M. B. Hursthouse, *J. Chem. Soc., Dalton Trans.*, 1992, 19.
- 9 J. B. Vincent, H.-L. Tsai, A. G. Blackman, S. Wang, P. D. W. Boyd, K. Folting, J. C. Huffman, E. B. Lobkovsky, D. N. Hendrickson and G. Christou, *J. Am. Chem. Soc.*, 1993, **115**, 12353.
- 10 R. Sessoli, H.-L. Tsai, A. R. Schake, S. Wang, J. B. Vincent, K. Folting, D. Gatteschi, G. Christou and D. N. Hendrickson, *J. Am. Chem. Soc.*, 1993, **115**, 1804.
- 11 H. J. Eppley, H.-L. Tsai, N. de Vries, K. Folting, G. Christou and D. N. Hendrickson, *J. Am. Chem. Soc.*, 1995, **117**, 301.
- 12 A. Caneschi, D. Gatteschi, R. Sessoli, A. L. Barra, L. C. Brunel and M. Guillot, *J. Am. Chem. Soc.*, 1991, **113**, 5873; R. Sessoli, D. Gatteschi, A. Caneschi and M. A. Novak, *Nature*, 1993, **365**, 141.
- 13 H.-L. Tsai, M. W. Wemple, D. M. Adams, G. Christou and D. N. Hendrickson, manuscript in preparation.